Noname manuscript No.
(will be inserted by the editor)

Passive SCR: The effect of H_2 to NO ratio on the formation of NH_3 over alumina supported platinum and palladium catalysts

Emma Catherine Adams · Magnus Skoglundh · Pär Gabrielsson · Per-Anders Carlsson

Received: date / Accepted: date

Abstract We investigate the relationship between the H_2:NO ratio and NH_3 formation over alumina supported Pt and Pd catalysts. By kinetic studies and *in situ* infrared spectroscopy, we report that NH_3 formation is not only sensitive to the catalyst formulation but equally dependent on the feed gas composition and temperature. Specifically, we identify that hydrogen plays an important role in the dissociation of NO at low temperature. We also show that the support material itself plays a vital role in the ammonia formation mechanism due to the redox behaviour of NO adsorption at low temperature. This was unexpected as the noble metal is generally considered to be the active phase for the reaction of NO and H_2.

Keywords Passive SCR · DRIFT spectroscopy · NH_3 formation

1 Introduction

Passive selective catalytic reduction (Passive-SCR) is a newly emerging technique for NO_x abatement in lean-burn SI gasoline passenger vehicles. This technology aims to utilise unwanted NO_x by reaction with hydrogen containing molecules present in the exhaust to provide an onboard supply of NH_3 [1–3]. This will reduce the dependence on an externally stored reductant, i.e. urea, as is currently preferred by heavy-duty NH_3-SCR technology for the reduction of NO_x to N_2 in the presence of excess O_2 [4–6]. The formed NH_3 can subsequently be stored down-stream on an SCR catalyst and be utilised as a reducing agent for NO_x during lean operation [1–3].

Two prominent routes for NH_3 formation using NO are reported in literature; the direct reaction of NO with H_2 and the hydrolysis of surface-bound isocyanate groups [7]. Focussing on the first route, which is the simpler of these two mechanisms, an understanding of how the ratio between the two reactants (H_2 and NO) affects the selectivity to NH_3 is of great interest. Previously, Xu *et al.* [8] have investigated the change in selectivity to N_2O, N_2 and NH_3 as a result of altering the [H_2]:[NO] ratio of the gas feed over Pt/Al_2O_3 and $Pt/BaO/Al_2O_3$. The authors observed that, at a catalyst temperature of 100 °C, a 100 % selectivity to NH_3 could be achieved when the H_2:NO ratio exceeded 2.5. However, the primary focus of their investigation was to develop and validate a mechanistic-based kinetic model for the reaction of NO with H_2 over Pt.

Since passive-SCR is a new field, a bottom-up approach to understand how to formulate suitable ammonia formation catalysts (AFC) is beneficial. Therefore, the aim of this paper is to investigate simple noble metal-support systems in order to add to the understanding of the differing steady-state selectivities observed during reaction of NO with H_2 at varying H_2:NO ratios. We do this by studying both low- and high-temperature steady-state effects, as well as conducting an *in situ* infrared investigation to identify and follow the evolution of surface species that are present during reaction.

E.C.Adams
emma.adams@chalmers.se

E.C.Adams, M.Skoglundh and P-A.Carlsson
Competence Centre for Catalysis
Chalmers University of Technology
SE-412 96 Göteborg
Sweden

P.Gabrielsson
Haldor Topsøe A/S
P.O Box 213
DK-2800 Lyngby
Denmark

We report on both Pt/Al_2O_3 and Pd/Al_2O_3 systems to determine how the active phase affects the reaction selectivity.

2 Experimental

2.1 Sample preparation

Alumina supported Pt (1.0 wt.%) and Pd (0.5 wt.%) powder catalysts were prepared by impregnating an alumina support (Puralox SBa200, SASOL) with grain size, d_{50} = 45 μm, pore volume = 0.35 - 0.50 ml/g and pore radius = 4 - 10 nm with an aqueous solution of platinum and palladium nitrate, respectively, using the incipent wetness impregnation technique. The synthesis method and monolith-coating procedure have been described in detail elsewhere [9]. Detailed characteristics of the samples including specific surface area, noble-metal particle size and precise metal-content are also reported therein. Although the noble-metal particle size range was determined as 2 - 21 nm for the Pt-containing sample, it was not possible to determine the corresponding particle size of the Pd/Al_2O_3 due to low contrast/resolution. However, the presence of Pd was confirmed by inductively coupled plasma optical emission spectroscopy and energy dispersive spectroscopic analyses.

2.2 Kinetic Analysis

Continuous gas flow reactor studies were conducted in order to determine how the ratio between NO and H_2 in the feed affects the formation of NH_3 and N-containing byproducts in the absence of O_2. The reactor setup employed in this investigation has previously been described by Kannisto *et al.* [10]. The inlet gas composition was controlled using mass flow controllers (Bronkhorst Hi-Tech LOW-ΔP-FLOW) and the outlet gas composition was analysed using FTIR spectroscopy (MKS 2030 HS). All experiments were carried out with an Ar balance in order to keep the total gas flow constant at 2000 ml/min, corresponding to a space velocity (GHSV) of 40 000 h^{-1}. Initially, the influence of H_2 was investigated by increasing the concentration of H_2 from 200 to 1500 ppm in 100 ppm steps, whilst the concentration of NO remained constant at 500 ppm. An additional step where the H_2 concentration is equal to 1250 ppm was included since high selectivity towards NH_3 has been reported when the stoichiometric requirement of H_2 is fulfilled, i.e H_2:NO >2.5 [8]. To ensure steady-state conditions, each data point was collected for 15 minutes. The experiments were conducted at 150 and 350 °C with the goal of distinguishing the dominating reaction pathway for the different rate limiting processes. The same temperature and time conditions as described for the H_2 dependence scheme were used for determining how NO affects the NH_3 formation. For these experiments, the H_2 concentration was kept constant at 1500 ppm whilst the concentration of NO was varied between 100 and 1500 ppm, again in steps of 100 ppm. An extra measurement point was added where the NO concentration was equal to 650 ppm.

2.3 Surface speciation

To follow the evolution of surface species during reaction, Infrared Fourier transform spectroscopy was carried out *in situ* in diffuse reflection mode (DRIFTS) using a Biorad FTS6000 spectrometer equipped with an *in situ* Harrick Praying Mantis reaction cell mounted with KBr windows. The effect of varying NO and H_2 concentration was investigated by following the time-resolved evolution of surface species during NH_3 formation. The gas composition was controlled via separate mass flow controllers (Bronkhorst Hi-Tech LOW-ΔP-FLOW) and an Ar balance was employed to maintain the 100 ml/min total gas flow fed to the reaction cell. As with the continuous gas flow reactor experiments, reactions were carried out at 150 and 350 °C and each spectrum was recorded at steady-state after 15 minutes of exposure to the feed gas. The NO concentration was kept constant at 500 ppm and the concentration of H_2 was varied between 0 and 1500 ppm, this time in steps of 200 ppm.
The temperature and time protocols described above were replicated for these experiments. The concentration of H_2 was held constant at 1500 ppm whilst that of NO was varied between 0 and 1400 ppm in steps of 50 - 300 ppm.

3 Results and Discussion

The effect of altering the amount of H_2 available for steady state NH_3 formation can be seen in Figure 1a. In all cases a steady increase in the generation of NH_3 is observed as the H_2 concentration of the feed gas increases. This occurs until the H_2 concentration is equal to approximately 1200 ppm ($[H_2]$:[NO] = 2.4), after which the concentration of formed NH_3 remains constant. The maximum possible concentration of formed NH_3 (500 ppm) is achieved when the reaction is carried out at 350 °C, whereas conversions of $\sim$ 50 % are observed under low-temperature conditions. An interesting observation is the difference in H_2-dependence

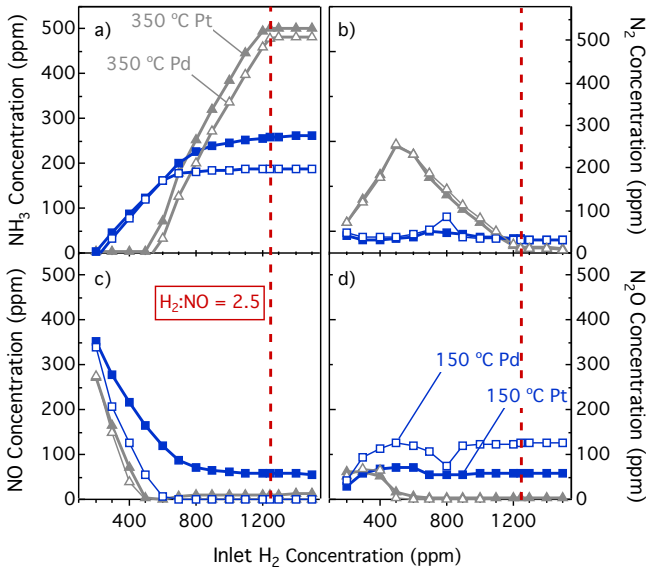

Fig. 1 Steady state formation of N_2, N_2O and NO over Pd/Al_2O_3 (open-markers) and Pt/Al_2O_3 (filled-markers) at 150 and 350 °C versus either the concentration of NO steps whilst H_2 concentration is kept constant at 1500 ppm, or the concentration of H_2 steps whilst NO is held constant at 500 ppm (Ar balance, GHSV = 40,000 h-1).

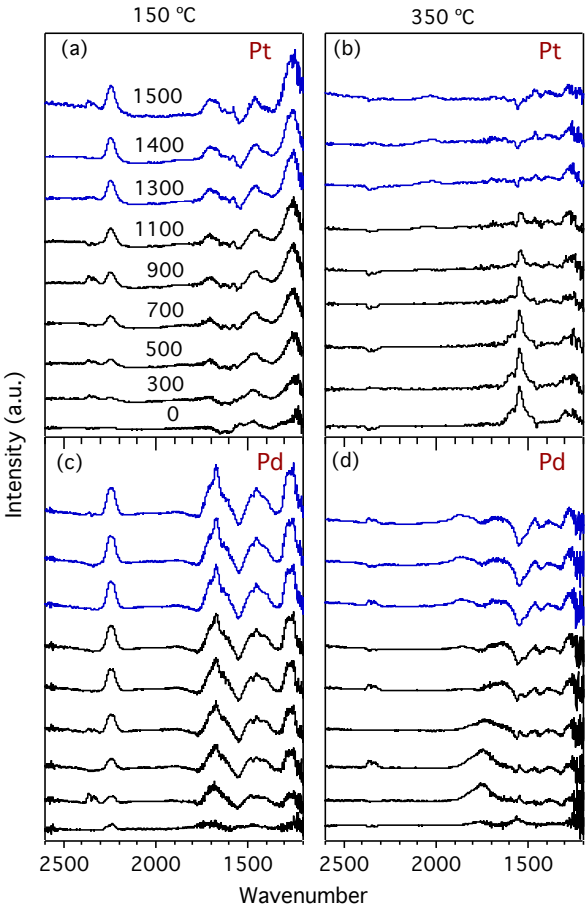

Fig. 2 DRIFTS spectra acquired during H_2 dependence experiments (H_2 concentration (ppm) of feed gas displayed on spectra). Top and bottom panels show surface species present on Pt/Al_2O_3 and Pd/Al_2O_3 respectively. The left panel shows the results of performing the experiment at low temperature (150 °C), whilst the right-hand panel shows results at 350 °C. NO concentration was constant at 500 ppm and Ar balance was employed to keep the total flow at 100 ml/min. Blue spectra show an $[H_2]$:[NO] >2.5

behaviour seen between low- and high-temperature conditions centred around the step where H_2 is equal to 700 ppm. When the H_2 concentration is below 700 ppm, low temperature is preferrable for NH_3 formation. At 350 °C, when no NH_3 formation is observed, Figures 1b and c show that the formation of N_2 steadily increases as the NO slip decreases. As N_2 could not be directly measured and no NO_2 is detected in the reactor outlet during any of these experiments, a nitrogen balance was used to calculate the formed amounts of N_2 according to the following equation:

$$N_2 = {}^1/_2NO_{inlet} - (N_2O + {}^1/_2NH_3 + {}^1/_2NO_{outlet})$$

Additionally when the H_2 concentration is below 700 ppm, a small contribution from N_2O is observed in Figure 1d which becomes negligible when H_2 is increased beyond this concentration. Conversely, when the H_2 concentration is above 700 ppm, higher temperatures are preferred for reaction of NO to NH_3. Consequently, the formation of N_2 steadily decreases and the NO slip becomes negligible. Overall, the differences in N-product selectivity obtained as a result of varying the H_2 composition of the feed gas at 350 °C agree with observations previously reported on Pt/Al_2O_3 by Xu *et al.* [8]. We also show that similar behaviour is exhibited by Pd-containing samples. The difference in selectivity to nitrogen-containing products as a result of varying the [NO]:$[H_2]$ ratio is found to correlate directly to the stoichiometric equations displayed below (eqn 1-3). These trends in selectivity over noble-metal systems correspond with findings reported in the 1970s when the suppression of NH_3 formation was of interest during early three-way catalyst (TWC) development [11, 12].

$$2NO + H_2 \rightarrow N_2O + H_2O \quad (1)$$

$$2NO + 2H_2 \rightarrow N_2 + 2H_2O \quad (2)$$

$$2NO + 5H_2 \rightarrow 2NH_3 + 2H_2O \quad (3)$$

The low activity for NH_3 formation exhibited at 150 °C might be due to a self-poisoning of the catalyst surface by NO, leading to a decreased availability of active sites for dissociative adsorption of H_2.

Upon observation of the DRIFT spectra displayed in Figure 2 (all peak assignments and references are found in Table 1), it can be seen that peaks representative of N-containing surface species (1400 - 1850 cm^{-1}) are much more prominent when the experiment is carried out at 150 (a and c) than 350 °C (b and d). Even more distinct however, is the peak at 2250 cm^{-1} which is only observed at low temperature and increases with increasing H_2 availability. In the literature, this peak has been frequently ascribed to isocyanate species, which are known to be an intermediate species that can be hydrolysed to form NH_3 [4,13,14]. However, since there is no CO present in the feed, this suggestion can be ruled out. Other species reported to be present at this wavenumber include NO^+ ions adsorbed on Al_2O_3 supported catalysts [15,16] and also gaseous N_2O [17,18]. During low-temperature reaction, we observe in Figure 1d, that a constant formation of N_2O is obtained throughout the experiment which seems to be unaffected by the H_2 concentration. Furthermore, the peak position is unaffected by varying the NO/H_2 ratios and no rotational bands are observed. Thus, to ascribe the growing absorption peak at 2250 cm^{-1} to N_2O would not be logical and so we conclude that this peak is due to the presence of NO^+ species on the alumina surface. This observation indicates a redox interaction between NO and the alumina support since no oxygen is present within the feed gas. The NO molecule is known to be a weak electron donor due to the presence of an unpaired electron in its configuration. Thus, upon coordination to a Lewis acid site on the alumina support, a partial charge transfer occurs, resulting in the partial oxidation of the NO molecule whilst the alumina support becomes partially reduced [19]. The implications of the increasing intensity of NO^+ and nitrate species as a result of increasing the $[H_2]$:[NO] ratio of the feed gas are two-fold; Firstly, we conclude that a reduced surface is the preferred state for NO adsorption to take place since minimal NO and nitrate peaks are observed when only NO is supplied in the feed. The pretreatment of the catalyst involved flowing oxygen over the sample at high temperature prior to switching to pure Ar for a short period in order to remove any carbonaceous surface contaminants from the material. O_2 was chosen for the pretreatment conditioning because the effect of H_2 was being investigated and it was important to have an H-free surface at the start of the experiment. We therefore assume that the Pt and Pd sites are initially present in an oxidized state when only NO is available in the feed and NO adsorption is negligible. Secondly, the growing intensity of the NO^+ peak at low temperature, coupled with the low activity for NH_3 formation (in comparison to the reaction carried out at 350 °C) indicates that a high surface coverage by NO limits the formation of NH_3. This will be further discussed below, where the concentration of NO provided to the reaction mixture reaches significant excess.

Table 1 Summary of species assignments for the *in situ* DRIFTS experiments.

Wavenumber (cm^{-1})	Species	Ref.
1273	NH_4^+ on Bronsted acid sites	[20,18]
1460	Linearly bound NO^{3-} on Al_2O_3	[20,21]
1496	Bridge-bonded NO^{3-} on Pd	[20]
1590	Chelating bidentate NO^{3-} on Al_2O_3	[20,22]
1610	Bridge-bonded bidentate NO^{3-} on Al_2O_3	[20,22]
1668	Linearly bound NO on Pt	[23]
1746	Linearly bound NO on Pd^0	[4,24]
1828	Linearly bound NO on Pd^+	[4,24]

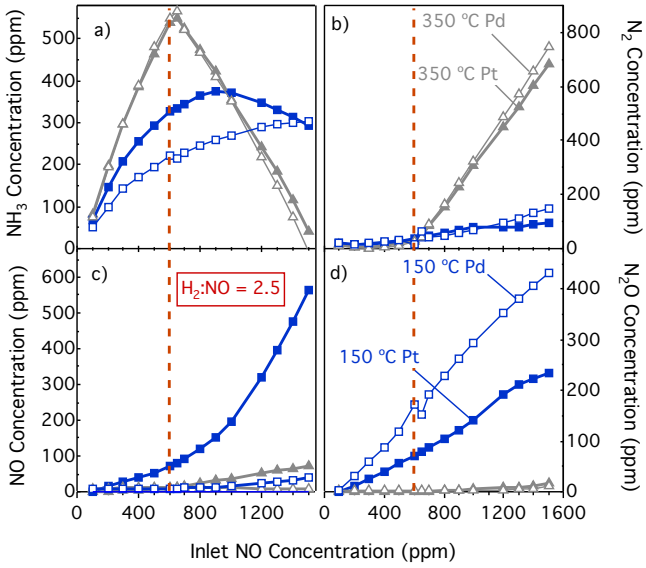

Fig. 3 Steady state formation of NH_3 over Pd/Al_2O_3 (open-markers) and Pt/Al_2O_3 (filled-markers) at 150 and 350 °C versus (a) the concentration of NO steps whilst H_2 concentration is kept constant at 1500 ppm, (b) the concentration of H_2 steps whilst NO is held constant at 500 ppm (Ar balance, GHSV = 40,000 h-1).

The effect of varying the NO concentration on the steady-state formation of NH_3 at constant H_2 concentration can be seen in Figure 3a. When performed at 350 °C, 100 % conversion of NO to NH_3 is achieved when the concentration of NO in the feed gas is varied between 100 and 600 ppm and the reaction appears

first order with respect to [NO]. This means that the ratio between the H_2 and NO concentrations in the feed gas is equal to or in excess of 2.5:1. As the concentration of NO available for reaction is increased beyond this point, the selectivity to NH_3 is negatively affected, most notably when the reaction is carried out at 350 °C. This rapid loss of NH_3 selectivity is accompanied by increasing generation of N_2, observed in Figure 3b. When exposed to low-temperature conditions (150 °C) considerable amounts of N_2O, exhibited in Figure 3d, are formed over both catalysts. An interesting difference in behaviour between Pt and Pd is observed when the reaction is carried out at 150 °C; At this temperature, the Pd- containing sample shows a steady increase in NH_3 formation throughout the entire experiment, whereas the Pt- containing sample exhibits a loss in activity when the NO concentration exceeds 1000 ppm. Figure 3c shows that this is due to an increase in NO slip over the Pt/Al_2O_3 which is not observed over Pd/Al_2O_3.
Upon observation of the obtained DRIFT spectra in Figure 4, we again see that the intensities of peaks representative of adsorbed NO and nitrate groups are higher during low-temperature conditions (a and c) than at high temperature (b and d). However, the contribution of these peaks is not as significant as when an excess of H_2 is available in the feed. The difference of the behaviour on the Pd/Al_2O_3 sample during this reaction compared to the H_2 dependence experiment is also of interest. When H_2 is available in excess, an increase in the amount of NO^+ species adsorbed on the catalyst surface is seen. However, only a very small contribution from this peak is observed when the concentration of NO is increased and the H_2 concentration remains constant. On the contrary, when the NO concentration of the feed is increased over Pt/Al_2O_3, the intensity of the NO^+ peak significantly increases, as for the case with the H_2 dependence reaction. Farberow *et al.* [25] have investigated the reaction of NO with H_2 over Pt(111) using DFT calculations, specifically focussing on the difference between NO surface coverage effects at high- and low-temperature. They found that the elementary step most affected by the degree of surface coverage by NO is the dissociation of NO on the active sites of the catalyst. At low temperature, the activation energy for this reaction increases from 2.32 eV on a clean Pt surface to 3.52 eV on a surface with high NO coverage. Similarly, Huai *et al.* [26] report an activation energy of 2.36 eV for the dissociative adsorption of NO on clean Pd (111). Therefore, it is assumed by both groups that for NO to dissociate, an intermediate pathway via formation of HNO prior to N-O bond scission is a more energetically favourable route. De Wolf *et al.* [27] also report that the presence of H_2 promotes

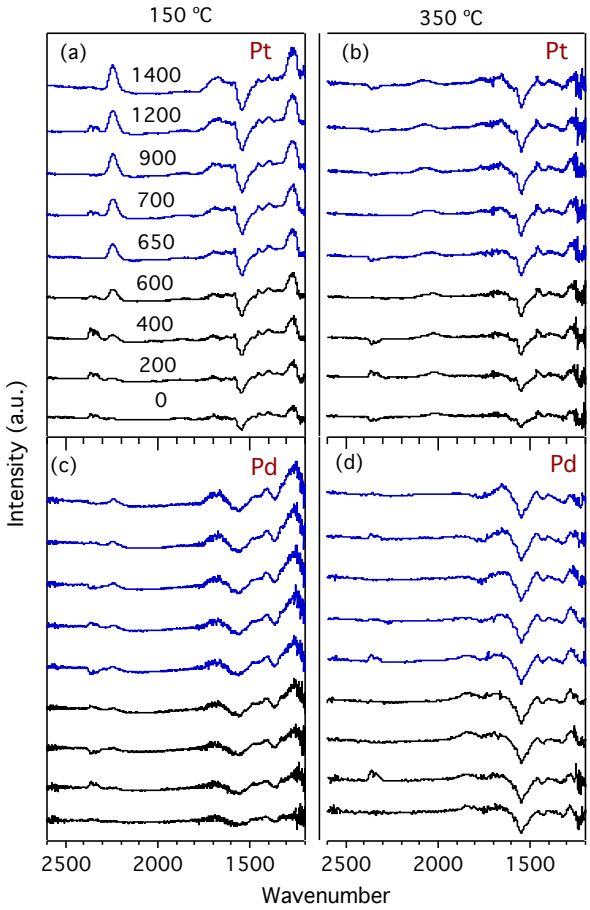

Fig. 4 DRIFTS spectra acquired during NO dependence experiments (NO concentration (ppm) of feed gas displayed on spectra). Top and bottom panels show surface species present on Pt/Al_2O_3 and Pd/Al_2O_3 respectively. The left panel shows the results of performing the experiment at low temperature (150 °C), whilst the right-hand panel shows results at 350 °C. H_2 concentration was constant at 1500 ppm and Ar balance was employed to keep the total flow at 100 ml/min. Blue spectra show an $[H_2]$:[NO] <2.5

the dissociation of NO and that any excess availability of H_2 subsequently contributes to the production of NH_3. This could explain the decrease in NH_3 selectivity and increase in N_2, N_2O and NO slip observed during both reaction protocols when the H_2:NO ratio of the feed is lower than the stoichiometric value of 2.5. Although there may be enough H_2 available to dissociate the adsorbed NO at low temperature, there is not a high enough presence to also react with the N adatoms and so surface recombination of the N and O is preferred.

4 Conclusions

We show that for the reaction of NO with H_2 over alumina supported Pt and Pd catalysts at intermediate

temperature, the selectivity to N-containing products follows the stoichiometry (eqns 1-3). Therefore, it is possible to achieve full conversion to NH_3 over these materials when the H_2:NO ratio is higher than 2.5. We also show that under low temperature conditions (150 °C), hydrogen is required to facilitate the dissociation of adsorbed NO, therefore reducing the effect of NO poisoning on the catalyst surface. Further, chemical processes on the alumina support itself are involved in the NH_3 formation mechanism due to the observed redox behaviour upon adsorption of NO.

5 Acknowledgements

This work was financially supported by the Swedish Energy Administration through the FFI program and the Competence Centre for Catalysis, which is financially supported by Chalmers University of Technology, the Swedish Energy Agency and the member companies: AB Volvo, ECAPS AB, Haldor Topsøe A/S, Volvo Car Corporation, Scania CV AB, and Wärtsilä Finland Oy.

References

1. C. D. DiGulio, J. A. Pihl, J. E. Parks II, M. D. Amiridis, and T. J. Toops *Catal. Today*, vol. 231, pp. 33–45, 2014.
2. V. Y. Prikhodko, J. E. Parks, J. A. Pihl, and T. J. Toops *SAE Int. J. Engines*, vol. 7, pp. 1235–1243, 2014.
3. S. H. Oh and T. Triplett *Catal. Today*, vol. 231, pp. 22–32, 2014.
4. N. Macleod, R. Cropley, J. M. Keel, and R. M. Lambert *J. Catal.*, vol. 221, pp. 20–31, 2004.
5. P. Balle, B. Geiger, D. Klukowski, M. Pignatelli, S. Wohnrau, M. Menzel, I. Zirkwa, G. Brunklaus, and S. Kureti *Appl. Catal. B: Environ.*, vol. 91, pp. 587–595, 2009.
6. Y. S. Cho, S. W. Lee, W. C. Choi, and Y. B. Yoon *Int. J. Automot. Techn.*, vol. 15, pp. 723–731, 2014.
7. F. Can, X. Courtois, S. Royer, G. Blanchard, S. Rousseau, and D. Duprez *Catal. Today*, vol. 197, pp. 144–154, 2012.
8. J. Xu, R. Clayton, V. Balakotaiah, and M. P. Harolk *Appl. Catal. B: Environ*, vol. 77, pp. 395–408, 2008.
9. E. C. Adams, M. Skoglundh, M. Folic, E. C. Bendixen, P. Garbrielsson, and P.-A. Carlsson *Appl. Catal. B: Environ*, vol. 165, pp. 10–19, 2015.
10. H. Kannisto, X. Karatzas, J. Edvardsson, L. J. Pettersson, and H. H. Ingelston *Appl. Catal. B: Environ.*, vol. 104, pp. 74–83, 2011.
11. H. G. Stenger Jr and J. S. Hepburn *Energy Fuels 1*, vol. 5, pp. 412–416, 1987.
12. T. P. Kobylinski and B. W. Taylor *J. Catal.*, vol. 33, pp. 376–384, 1974.
13. K. Almusaiteer and S. C. Chuang *J. Catal.*, vol. 180, pp. 161–170, 1998.
14. N. Macleod and R. M. Lambert *Appl. Catal. B: Environ.*, vol. 46, pp. 483–495, 2003.
15. A. Iglesias-Juez, A. B. Hungría, A. Martínez-Arias, A. Fuerte, M. Fernández-García, J. A. Anderson, J. C. Conesa, and J. Soria *J. Catal.*, vol. 217, pp. 310–323, 2003.
16. B. C. Hixson, J. W. Jordan, E. L. Wagner, and H. M. Bevsek *J. Phys. Chem. A*, vol. 115, pp. 13364–13369, 2011.
17. J.-B. Yang, O.-Z. Fu, D.-Y. Yong, and S.-D. Wang *Appl. Catal. B: Environ.*, vol. 49, pp. 61–65, 2004.
18. C. Neyertz, D. Volpe, D. Perez, I. Costilla, M. Sanchez, and C. Gigola *Appl. Catal. A: Gen.*, vol. 368, pp. 146–157, 2009.
19. K. Hadjiivanov, J. Saussey, J. L. Freysz, and J. C. Lavalley *Catal. Lett.*, vol. 1998, pp. 103–108, 1998.
20. T. J. Toops, D. B. Smith, W. S. Epling, J. E. Parks, and W. P. Partridge *Appl. Catal. B: Environ.*, vol. 58, pp. 255–264, 2005.
21. W. S. Kijlstra, D. S. Brand, E. K. Poels, and A. Bliek *J. Catal.*, vol. 171, pp. 208–218, 1997.
22. F. Prinetto, G. Ghiotti, I. Nova, L. Lietti, E. Tronconi, and P. Forzatti *J. Phys. Chem. B*, vol. 2001, pp. 12732–12745, 2001.
23. S.-H. Chien, M.-C. Kuo, C.-H. Lu, and K.-N. Lu *Catal. Today*, vol. 97, pp. 121 – 127, 2004.
24. D. D. Miller and S. S. C. Chuang *J. Taiwan Inst. Chem. E.*, vol. 40, pp. 613–621, 2009.
25. C. A. Farberow, J. A. Dumesic, and M. Mavrikakis *ACS Catal.*, vol. 4, pp. 3307–3319, 2014.
26. L.-Y. Huai, C.-Z. He, H. Wang, H. Wen, W.-C. Yi, and J.-Y. Liu *J. Catal.*, vol. 322, pp. 73–83, 2015.
27. C. A. de Wolf and B. E. Nieuwenhuys *Surf. Sci.*, vol. 469, pp. 196–203, 2000.